# Approximate Factorization Schemes for Three-Dimensional Nonlinear Supersonic Potential Flow

M. J. Siclari*
*Grumman Aerospace Corporation, Bethpage, New York*

**The nonconservative finite difference analog of the three-dimensional full-potential equation is solved implicitly by marching in a radial coordinate system with the marching initiated by a conical flow at the apex. The crossflow is a mixed type and transonic type-dependent differencing is used to determine each spherical plane solution. Two types of approximate factorizations are studied, the AF1 or ADI and the AF2 factorization. In the AF2 factorization, one of the second derivatives is split between the two factors. The type of AF2 factorization that was found to work for the conical problem was also found to be more sensitive to the coordinate transformations and strong shocks than the AF1 scheme. Both schemes were found to require some form of temporal damping for stability for the multishock conical flow problem. The AF1 factorization was then extended to include three-dimensional flows with the bow shock fit by explicitly including the hyperbolic third-dimension terms. The AF1 factorization was shown to improve the convergence rate markedly for most cases.**

## Introduction

THE numerical solution of supersonic flow problems using the full-potential equation has become an attractive and promising alternative to solving either Euler equations or the linearized potential flow equations. The full-potential equation retains most of the nonlinear features of the flowfield, such as shocks, that the linearized potential or the more popular linear panel methods inherently neglect, while having the simplicity of a single variable irrotational solution. Primitive variables, entropy singularities, and CFL stability conditions tend to complicate Euler equation solvers.[1] The current approach to supersonic flows was first established by Grossman[2] for the conical flow problem using a nonconservative form of the potential equation. The conical flow problem reduces the full-potential equation to an equation which, in the cross-flow plane (i.e., transverse plane normal to conical rays), contains all of the salient features of the two-dimensional transonic full-potential equation. In Ref. 2, it was found that because of the type-dependent, or mixed elliptic/hyperbolic, nature of the cross flow, transonic techniques such as those developed early by Jameson[3] could be used to determine numerical solutions. The conical flow problem was extended by Grossman and Siclari[4] to include three-dimensional flow using a fully implicit marching technique where each marching step requires an implicit cross-flow solution. These schemes have all used successive line-over-relaxation (SLOR) as their basis for numerical solution of the nonconservative full-potential equation. For the nonconical problem, it was found by Siclari[5] that accuracy could be enhanced by isentropically fitting the bow shock and numerical efficiency optimized by a judicious selection of the sweep direction. As the procedure for solving the full-potential equation for supersonic problems matured, other investigators established similar methods. Shankar et al.,[6,7] using a semi-implicit marching technique with a density linearization of the conservative full-potential equation, has also shown success. Comparisons of Shankar's conservative approach with the present nonconservative formulation in Ref. 6 have shown remarkably excellent agreement considering the conservative vs nonconservative treatments. The semi-implicit formulation of Ref. 6 or 7 requires some CFL constraints, unlike the present fully implicit formulation which has no CFL constraints. Sritharan[8] has also developed

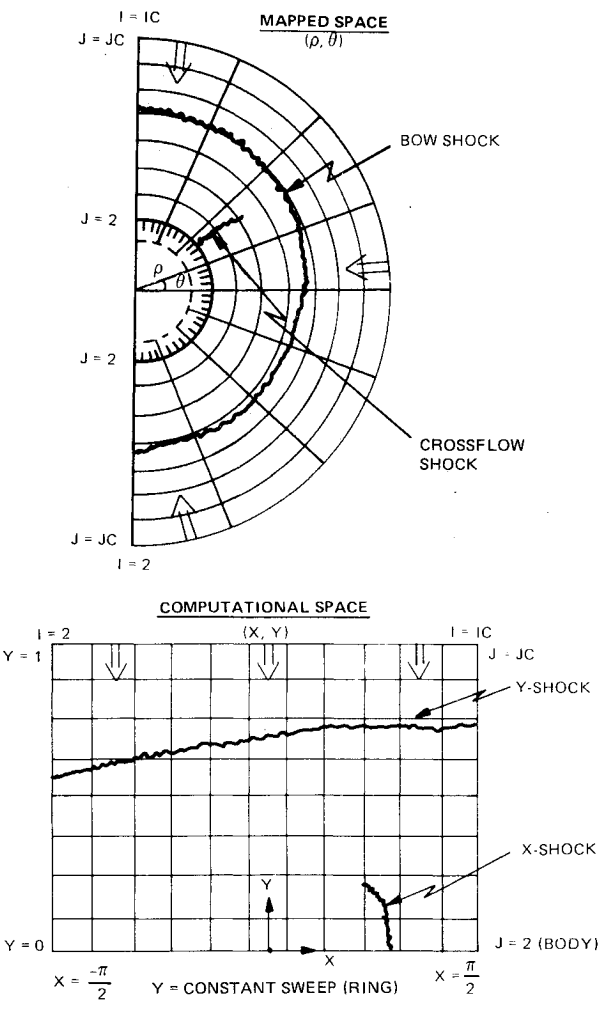


**Fig. 1 Sweep and mesh definitions.**

Presented as Paper 83-0376 at the AIAA 21st Aerospace Sciences Meeting, Reno, Nev., Jan. 10-13, 1983; received April 7, 1983; revision received March 1, 1984. 

*Staff Scientist, Research & Development Center.

a conservative formulation for solving the conical problem. Comparisons with the present approach shown in Ref. 8 exhibit excellent agreement, except for the typical conservative/nonconservative disparities that occur in the vicinity of the captured cross-flow shock.

In the present study, numerical techniques are investigated that show promise for accelerating convergence in comparison with the standard SLOR methods. The primary candidate for this is the alternating-direction-implicit (ADI)[9] or, as it is more commonly referred to in its application to transonic flows, approximate factorization (AF) schemes. These AF schemes have been applied successfully to a variety of transonic flow problems. Initially, AF schemes were applied to the transonic small-disturbance (TSD) equation by Ballhaus et al.[10] Holst[11] successfully applied an AF2 scheme to the conservative full-potential equation for transonic flows. The nonconservative full-potential equation was treated successfully by Baker[12,13] for two-dimensional transonic flows and should be applicable to the nonconservative full-potential supersonic/transonic cross-flow problem of the present study. Two basic AF algorithms are considered, ADI or AF1 and the AF2 scheme which splits one of the second derivatives into two first-order derivative operators. The lattermost scheme has been reported to be the most stable in supersonic flow regions for the transonic flow problem.

## Basic Formulation

The nonconservative form of the three-dimensional full-potential equation is written in a spherical coordinate system $(\omega,\psi,r)$. The governing equation is then transformed via a stereographic projection to $(p,q,t)$ coordinates and further by the cross-flow conformal mapping to $(\rho,\theta,R)$ coordinates. In terms of a reduced potential $F$, where $\vec{Q}=\nabla\varphi+\vec{q}\infty$, and $\varphi=RF(\rho,\theta,R)$, the principal terms of the three-dimensional full-potential equation can be written as:

$$\frac{(a^2-U^2)}{\rho^2}F_{\theta\theta}-\frac{2UV}{\rho}F_{\rho\theta}+(a^2-V^2)F_{\rho\rho}+\ldots$$
$$=RH\Big\{[(W^2-a^2)RHh_1+2WV]\left[h_1F_{\rho\rho}+\frac{h_2}{\rho}F_{\rho\theta}+F_{\rho R}\right]$$
$$+\frac{1}{\rho}[(W^2-a^2)RHh_2+2WU]\left[h_1F_{\rho\theta}+\frac{h_2}{\rho}F_{\theta\theta}+F_{\theta R}\right]$$
$$+RH(W^2-a^2)\left[h_1F_{\rho R}+\frac{h_2}{\rho}F_{\theta R}+F_{RR}\right]+\ldots\Big\} \qquad (1)$$

where $U$, $V$, and $W$ are the velocities in the $\theta$, $\rho$, and $R$ directions, respectively, and $H$ is the metric of the two mappings. In general, the conformal mapping in the cross-flow plane leads to a nonorthogonal coordinate system if the mapping singularity is a function of $r$. This mapping dependence on $r$ leads to mesh derivatives defined as $h_1=\rho_r$ and $h_2=\theta_r/\rho$. The radial marching direction $r$ remains unchanged due to the transformations, or $r=t=R$. The details of the mappings and coefficients can be found in Refs. 2 and 4.

Unlike transonic flow, the supersonic flow problem is contained within a finite cross-flow mesh bounded by a bow shock. The bow shock may be captured within a prescribed outer boundary[2,4] or can be fit as the outer boundary[5] using the isentropic shock jump conditions.

A shearing transformation is applied to Eq. 1 between the body $\rho=B(\theta,R)$ and the outer boundary or bow shock $\rho=C(\theta,R)$, where

$$X=\theta, \qquad Y=(\rho-B)/(C-B), \qquad Z=R \qquad (2)$$

which yields a final rectangular computational mesh.

Equation (1) can be represented as the sum of a conical plus a nonconical operator, in the form:

$$L(\varphi_{i,j})=L_C(\varphi_{i,j})+RL_{NC}(\varphi_{i,j}) \qquad (3)$$

The nonconical coefficients on the right-hand side of Eq. (1) all have an $R$ dependence and vanish identically at $R=0$ for the quasi-two-dimensional conical flow problem.

## Conical Flows

For conical flows, after applying the shearing transformation, Eq. (1) can be written as

$$L_C(\varphi_{i,j})=A_1F_{XX}+A_2F_{XY}+A_3F_{YY}+\ldots \qquad (4)$$

where

$$A_1=\frac{(a^2-U^2)}{\rho^2}$$
$$A_2=\frac{-2UV}{\rho}Y_\rho+\frac{2(a^2-U^2)}{\rho^2}Y_\theta$$
$$A_3=(a^2-V^2)Y_\rho^2-\frac{2UV}{\rho}Y_\rho Y_\theta+\frac{(a^2-U^2)}{\rho^2}Y_\theta^2 \qquad (5)$$

Equation (4) closely resembles the nonconservative form of the two-dimensional transonic flow equation. The difference is that the type dependency of the conical part of Eq. (1) or (4) is linked to the nature of the cross-flow velocity defined by $Q_c^2=U^2+V^2$. An upwind bias in the difference equations must occur when the cross-flow velocity is supersonic or $Q_c^2>a^2$. The cross-flow velocity component $V$ is always negative and toward the body surface. The $U$ component of velocity can be positive or negative depending upon the geometry and angle of attack. Heretofore, Eq. (4) has been solved successfully using transonic SLOR techniques[2,4] and the rotated difference scheme of Jameson.[3]

The principal part of Eq. (4) can be rewritten in a rotated difference format as, for $Q_c^2>a^2$,

$$A_1F_{XX}+A_2F_{XY}+A_3F_{YY}=(a^2-Q_c^2)F_{ss}+a^2F_{nn} \qquad (6)$$

where

$$F_{ss}=\frac{V_1^2}{Q_c^2}F_{YY}+\frac{2U_1V_1}{Q_c^2}F_{XY}+\frac{U_1^2}{Q_c^2}F_{XX}$$
$$F_{nn}=\frac{U_2^2}{Q_c^2}F_{YY}-\frac{2U_2V_2}{Q_c^2}F_{XY}+\frac{V_2^2}{Q_c^2}F_{XX}$$

and

$$U_1=U/\rho, \qquad V_1=VY_\rho+(UY_\theta/\rho)$$
$$V_2=V/\rho, \qquad U_2=UY_\rho-(VY_\theta/\rho)$$

An upwind bias is applied to the finite difference representation of the $F_{ss}$ terms and central differences are used for the $F_{nn}$ terms in supersonic cross-flow regions.

The following sections will present an adaptation of the two basic AF algorithms, ADI or AF1 and AF2, to the present supersonic flow problem.

### AF1 Factorization

An ADI or AF1 type factorization can be applied to the principal terms of Eq. (4) for subsonic cross-flow $Q_c^2<a^2$ in the form:

$$\left(\alpha-A_1\frac{\vec{\delta}_X\overleftarrow{\delta}_X}{\Delta X^2}\right)\left(\alpha-A_3\frac{\vec{\delta}_Y\overleftarrow{\delta}_Y}{\Delta Y^2}\right)\Delta_{i,j}^{n+1}=\alpha\omega L_c(\varphi_{i,j}^n) \qquad (7)$$

where $\Delta_{i,j}$ is the correction to the reduced potential $F_{i,j}$ or $\Delta_{i,j}=F^{n+1}_{i,j}-F^{n}_{i,j}$. $\omega$ is a relaxation parameter and $L_c(\varphi_{i,j})$ the residual of Eq. (4) at the $n$th iteration. $\alpha$ is an acceleration parameter varied in a cyclic fashion during the iteration process. The two first-order difference operators result in a second-order central difference. The first-order operators are defined as

$$\vec{\delta}_X=(\ )_{i+1,j}-(\ )_{i,j}, \qquad \overleftarrow{\delta}_X=(\ )_{i-1,j}-(\ )_{i,j}$$
$$\vec{\delta}_Y=(\ )_{i,j+1}-(\ )_{i,j}, \qquad \overleftarrow{\delta}_Y=(\ )_{i,j}-(\ )_{i,j-1} \tag{8}$$

The basic premise behind an approximate factorization scheme can be revealed if the left-hand side of Eq. (7) is expanded and terms not resembling those of Eq. (4) are neglected, or

$$\left(A_1\frac{\vec{\delta}_X\overleftarrow{\delta}_X}{\Delta X^2}+A_3\frac{\vec{\delta}_Y\overleftarrow{\delta}_Y}{\Delta Y^2}\right)\Delta^{n+1}_{i,j}=-\omega L_c(\varphi^n_{i,j}) \tag{9}$$

If $\omega=1$, Eq. (9) would be equivalent to solving Eq. (4) with the cross derivative evaluated using old values of the potential. Equation (9) is typically solved in a two-step format by defining an intermediate variable, $G_{i,j}$, where

$$\left(\alpha-A_1\frac{\vec{\delta}_X\overleftarrow{\delta}_X}{\Delta X^2}\right)G^{n+1}_{i,j}=\alpha\omega L_c(\varphi^n_{i,j})$$
$$\left(\alpha-A_3\frac{\vec{\delta}_Y\overleftarrow{\delta}_Y}{\Delta Y^2}\right)\Delta^{n+1}_{i,j}=G^{n+1}_{i,j} \tag{10}$$

Equation (10) represents two tridiagonal systems of equations involving differences only in the computational $X$ or $Y$ direction. Equation (10) must be modified in regions of supersonic crossflow to include the proper upwind bias. The following form of the supersonic cross-flow factorization is essentially identical to the AF1 scheme of Baker[5,12] for the transonic nonconservative full-potential equation. Hence, for $Q_c^2>a^2$,

$$\left(\alpha-A_{1c}\frac{\vec{\delta}_X\overleftarrow{\delta}_X}{\Delta X^2}-K_1A_{1u}\frac{\overleftarrow{\delta}_X\overleftarrow{\delta}_X}{\Delta X^2}-K_2A_{1u}\frac{\vec{\delta}_X\vec{\delta}_X}{\Delta X^2}\right)G^{n+1}_{i,j}=\alpha\omega L(\varphi^n_{i,j})$$
$$\left(\alpha-A_{3c}\frac{\vec{\delta}_Y\overleftarrow{\delta}_Y}{\Delta Y^2}-A_{3u}\frac{\vec{\delta}_Y\vec{\delta}_Y}{\Delta Y^2}\right)\Delta^{n+1}_{i,j}=G^{n+1}_{i,j} \tag{11}$$

The central (subscript $c$) and upwind coefficients (subscript $u$) are given by the rotated difference scheme equation (6) as

$$A_{1c}=\frac{V_2^2}{Q_c^2}, \qquad A_{3c}=\frac{U_2^2}{Q_c^2}$$
$$A_{1u}=\frac{(a^2-Q_c^2)}{Q_c^2}U_1^2, \qquad A_{3u}=\frac{(a^2-Q_c^2)}{Q_c^2}V_1^2 \tag{12}$$

The first factor allows for the $U$ component of velocity to be positive or negative where, if

$$U>0, \quad K_1=1, \quad K_2=0$$
$$U<0, \quad K_1=0, \quad K_2=1 \tag{12a}$$

As mentioned earlier, the $V$ velocity is always negative for supersonic cross flow and, hence, only forward upwind differences occur in the second factor.

In general, the first factor involves a pentadiagonal matrix and the second factor a quadradiagonal matrix. As suggested by Baker,[12] these differences can be replaced by

$$\overleftarrow{\delta}_X\overleftarrow{\delta}_X=(\ )^{n+1}_{i,j}-(\ )^{n+1}_{i-1,j}-(\ )^{n}_{i-1,j}+(\ )^{n}_{i-2,j}$$
$$\vec{\delta}_X\vec{\delta}_X=(\ )^{n+1}_{i,j}-(\ )^{n+1}_{i+1,j}-(\ )^{n}_{i+1,j}+(\ )^{n}_{i+2,j}$$
$$\vec{\delta}_Y\vec{\delta}_Y=(\ )^{n+1}_{i,j}-(\ )^{n+1}_{i,j+1}-(\ )^{n}_{i,j+1}+(\ )^{n}_{i,j+2} \tag{13}$$

This reduces the set of Eq. (11) to the following tridiagonal form for $Q_c^2>a^2$:

$$\left[\alpha-A_{1c}\frac{\vec{\delta}_X\overleftarrow{\delta}_X}{\Delta X^2}-I_s\frac{A_{1u}}{\Delta X^2}(K_1\overleftarrow{\delta}_X+K_2\vec{\delta}_X)\right]G^{n+1}_{i,j}=\alpha\omega L_c(\varphi^n_{i,j})$$
$$\left(\alpha-A_{3c}\frac{\vec{\delta}_Y\overleftarrow{\delta}_Y}{\Delta Y^2}+\frac{A_{3u}\vec{\delta}_Y}{\Delta Y^2}\right)\Delta^{n+1}_{i,j}=G^{n+1}_{i,j} \tag{14}$$

where, for $U>0$, $I_s=1$ and $U<0$, $I_s=-1$.

**AF2 Factorization**

The AF2 algorithm has been found by several investigations[10,11] generally to be the more stable AF factorization for transonic flows. In the AF2 factorization, one of the second derivatives is split between the two factors. Following a similar AF2 factorization used by Baker[12] for subsonic crossflow $Q_c^2<a^2$, the AF2 algorithm becomes

$$\left(\frac{-\alpha}{H_m}\frac{\vec{\delta}_Y}{\Delta Y}-A_1\frac{\vec{\delta}_X\overleftarrow{\delta}_X}{\Delta X^2}\right)\left(\alpha+A_3H_m\frac{\overleftarrow{\delta}_Y}{\Delta Y}\right)\Delta^{n+1}_{i,j}=\alpha\omega L_c(\varphi^n_{i,j}) \tag{15}$$

This form of factorization is thought to be more stable since the $Y$ operator in the first factor yields a $\varphi_{Yt}$ term, unlike the $\varphi_t$ term of the AF1 scheme.[13] The term $H_m$ in the two factors accounts for the transformation derivatives of the mapped and sheared mesh. As illustrated by Catherall,[14] the proper splitting of these transformation derivatives can yield optimum convergence, and neglecting these derivatives can considerably degrade convergence. The coefficient $A_3$ in Eq. (4) contains the shearing transformation derivatives $Y_\rho$ and $Y_\theta/\rho$. The mapped plane $(\rho,\theta)$ velocities, $V$ and $U$, respectively, contain the metric $H(\rho,\theta)$ of the two mappings, Hence, a suitable form for the factor $H$ might be

$$H_m=\frac{\Delta Y}{\Delta X}\frac{Y_\rho}{H} \quad \text{or} \quad \frac{\Delta Y}{\Delta X}\frac{1}{H}\left(Y_\rho-\frac{Y_\theta}{\rho}\right) \tag{16}$$

The first-order forward difference operator on $Y$ is placed in the first factor since this term does not switch for supersonic cross-flow conditions. For supersonic cross flow, the AF2 factorization is modified to include an upwind bias and a tridiagonal form as

$$\left[\frac{-\alpha}{H_m}\frac{\vec{\delta}_Y}{\Delta Y}-A_{1c}\frac{\vec{\delta}_X\overleftarrow{\delta}_X}{\Delta X^2}-\frac{I_sA_{1u}}{\Delta X^2}(K_1\overleftarrow{\delta}_X+K_2\vec{\delta}_X)\right]G^{n+1}_{i,j}$$
$$=\alpha\omega L_c(\varphi^n_{i,j})$$
$$\left[\alpha+A_{3c}H_m\frac{\overleftarrow{\delta}_Y}{\Delta Y}+A_{3u}H_m\frac{\vec{\delta}_Y}{\Delta Y}\right]\Delta^{n+1}_{i,j}=G^{n+1}_{i,j} \tag{17}$$

Since the forward $Y$ operator is included in the first factor, the sweep is constrained to be toward the body surface or decreasing $J$.

An alternate factorization of the AF2 scheme described above would be to split the $X$ derivative. Unlike transonic flow, the difficulty in splitting the $X$ derivative in the supersonic problem is that the $U$ velocity in the supersonic

cross-flow region can be either positive or negative. This occurs primarily at the captured bow shock. In transonic flow, the $X$ or $U$ velocity direction is much like the $Y$ direction of the present problem in that a negative supersonic $U$ velocity is unlikely to occur. Hence, there is no first order $X$ operator that, in general, does not switch. One could propose a scheme where the factorization is set up for $U<0$, and, if $U>0$, the upwind coefficient is either neglected or a shift operator is imposed. This scheme was found to be unstable or would not work for this problem.

Other AF2 factorizations were considered, including the AF3 factorization of Baker[12] where both coefficients are brought into the first factor. This would seem to be a candidate for a faster scheme since the differential operators would not act on the coefficients and lead to spurious terms. Baker,[12] in fact, has reported his AF3 scheme to be considerably faster than either the AF1 or AF2 schemes. Unfortunately, this scheme could not be applied successfully to Eq. (17).

#### Boundary Conditions

Figure 1 illustrates the conformally mapped and sheared computational cross-flow plane domains. Symmetry conditions are imposed at $\theta=\pm\pi/2$ or $I=2$ and $IC$ for the symmetric half-plane problem. Hence, periodic end conditions apply on $Y=$const lines. On $X=$const lines, $J=2$ corresponds to the body surface, and $J=JMAX$ corresponds either to the outer boundary (BSC) or the bow shock (BSF). In both the bow shock capture or fit methods, the outer boundary has the same condition that the correction to the potential vanish, or

$$\Delta_{i,j\max}=0 \tag{18}$$

A dummy row or $Y=$const line at $J=1$ is used to implement the body boundary condition of flow tangency. This condition relates the values of the correction at $J=1$ to those at $J=3$, or, for conical flow, yields

$$\Delta_{i,1}=\Delta_{i,3} \tag{19}$$

In this way, central derivatives can be used for $F_Y$ and the body surface coordinate line can be treated like any other coordinate line.

The order of the factors in both AF schemes were chosen so that the first sweep is carried out on $Y=$const lines. This was chosen over the reverse factorization so that periodic end conditions could be imposed on the intermediate variable $G$, or

$$G_{1,j}=G_{3,j}, \qquad G_{IC+1,j}=G_{IC-1,j} \tag{20}$$

which most certainly is a reasonable assumption. If the factors in the AF schemes are reversed, then somewhat arbitrary boundary conditions must be imposed on the intermediate variable $G$. The end conditions (18) and (19) then apply to the second sweep on the $X=$const lines.

#### Temporal Damping

It has been indicated that the basic AF1 scheme may be unstable in supersonic regions. To allow for this possibility, the AF1 scheme has been generalized to include an explicit temporal damping $F_{st}$ (e.g., $\varphi_{st}$) term. Jameson's generalized AF scheme[15] includes similar terms in both factors. In Ref. 11, it was indicated that this term may also be required in the AF2 scheme. It was found that adding this term explicitly to the first factor was sufficient to maintain stability for flows with captured shocks. This stability or temporal damping term has the form[5]:

$$-\epsilon\delta_{st}=-\epsilon\left[\frac{V_I}{Q_c}\vec{\delta}_Y+\frac{U_I}{Q_c}\left(K_I\overleftarrow{\delta}_X+K_2\vec{\delta}_X\right)\right]$$

where

$$\frac{K}{|1-M_c|}\le\epsilon\le\epsilon_{\max}K, \qquad \epsilon_{\max}=10 \tag{21}$$

In general, the addition of the temporal damping slows convergence. Hence, the form of the factor $\epsilon$ was chosen to maximize the damping in the vicinity of sonic lines or across shocks so as not to cause an overall degeneration in the convergence rate. The constant $K$ is chosen to be as small as possible for the optimum convergence.

In general, there are no restrictions on the sweep due to the velocity directions in an AF1 scheme. The first sweep can be from the outer boundary to the body surface or the reverse. In order to properly include temporal damping in the AF1 scheme, the first sweep must be in the direction of the supersonic crossflow. This requires that the $Y=$const sweep must be toward the body or decreasing $J$ since $V<0$.

It was observed that the AF1 scheme required little or no temporal damping, except for the most difficult cases, whereas the AF2 scheme required considerably higher values of $\epsilon$ for the strong $Y$-shock solutions.

#### Acceleration Parameter

For the AF1 scheme, the maximum and minimum values of the acceleration parameter $\alpha$ were taken as

$$\alpha_{\max}=A_{\max}\left(\frac{1}{\Delta X^2}+\frac{1}{\Delta Y^2}\right)$$

$$\alpha_{\min}=A_{\min}\left(\frac{1}{\Delta X}+\frac{1}{\Delta Y}\right) \tag{22}$$

The coefficients $A_{\min}$ and $A_{\max}$ were taken anywhere from 0.5 to 4.0 for all of the cases computed in this paper. The convergence rate could be affected by as much as a factor of 2 by a judicious choice of these parameters.

In the AF2 scheme, these parameters were chosen as

$$\alpha_{\max}=A_{\max}\left(\frac{1}{\Delta X}+\frac{1}{\Delta Y}\right)$$

$$\alpha_{\min}=A_{\min}\left(\frac{1}{\Delta X}+\frac{1}{\Delta Y}\right) \tag{23}$$

where $A_{\min}$ varied between 0.5 and 6 and $A_{\max}$ between 3 and 6. Typically, unity for $A_{\min}$ and 3 for $A_{\max}$ was sufficient for most cases. The theoretical value of $\alpha_{\min}=1$ or 2 could never be achieved possibly due to the effect of the various coordinate transformations.

For both AF schemes, the cyclic variation of $\alpha$ took the form:

$$\alpha_I=\alpha_{\max}\left(\frac{\alpha_{\min}}{\alpha_{\max}}\right)^{\left(\frac{I-1}{JMAX-1}\right)} \quad \text{for } I=1, JMAX \tag{24}$$

where $JMAX=3$ for the AF1 scheme and $JMAX=6$ for the AF2 scheme. The minimum number of cycles seemed to be the best choice for the AF1 scheme. The convergence rate of the AF2 scheme was affected insignificantly for $JMAX$ between 3 and 6. Further increase in $JMAX$ reduced the convergence rate. In all of the cases computed $\omega_{AF1}=1.50$ and $\omega_{AF2}=1.33$. Departures from Eq. (24) did not seem to affect the convergence rates significantly.

## Conical Results

Two techniques are available for the computation of supersonic conical flows, the bow shock capture[2,4] (BSC), and bow shock fit[5] (BSF) methods. In the BSC method, an outer mesh boundary, $\rho=C(\theta)$, is prescribed and the bow shock is captured within this boundary. The BSC method is a more

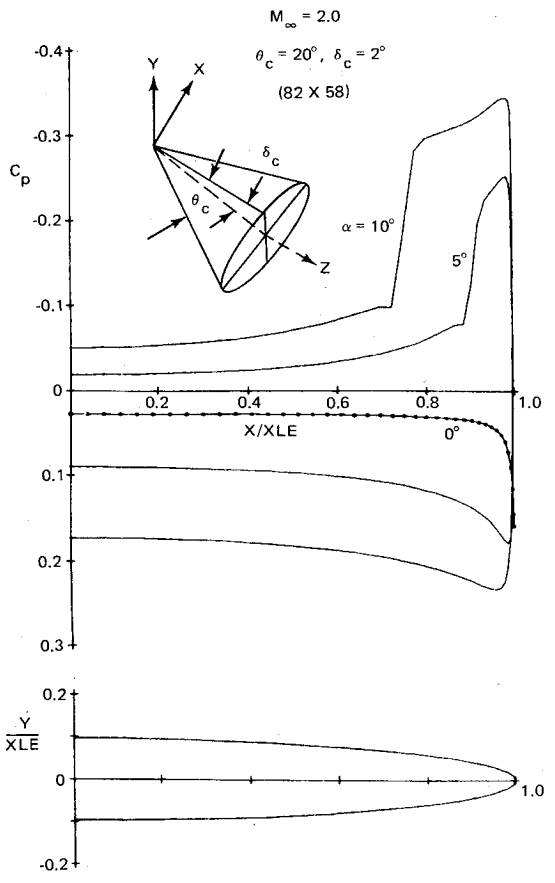


Fig. 2 Effect of surface boundary condition and factor sequence on the AF1 scheme (BSC) convergence rate.

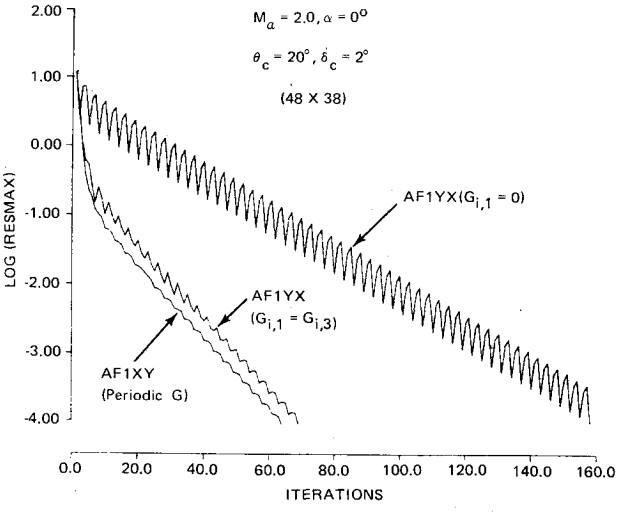


Fig. 3 Comparison of AF1 convergence rate with SLOR (BSC).

stringent test of the AF schemes in that two shocks may be present in the flow, the bow shock ($Y$ shock), and an embedded cross-flow shock ($X$ shock) as illustrated in Fig. 1. The bow shock is the most critical because its position and strength largely determine the internal flow. The bow shock also extends around the entire field encompassing more points than the embedded cross-flow shock. The BSF method fits the bow shock as the outer boundary and, hence, eliminates the bow shock from the internal flow calculation; and, if an embedded supersonic cross-flow region is not present, the internal flow problem becomes elliptic. The conical convergence rate of the BSF method is largely determined by the implicit shock fitting procedure where the shape of the boundary is updated and usually underrelaxed until the isentropic shock jump condition is fulfilled at each shock mesh point. The conical BSF method also requires more computational time per iteration because the cross-flow mesh and metrics must be recomputed for each iteration after the bow shock shape has been updated.

For conical flow, the BSC method is used primarily to evaluate the AF schemes. Figure 2 shows the effect of reversing the order of the factors in the AF1 scheme for a thin elliptic cone at $M_\infty = 2.0$, $\alpha = 0$ deg. The AF1XY scheme represents the order of the factors indicated in Eqs. (7) and (14) where periodic end conditions are used for the intermediate variable $G$. The factors were then reversed (AF1YX) with the first sweep occurring on $X = \text{const}$ lines. Two different boundary conditions were used: setting $G_{i,1} = 0$ as the end condition in the tridiagonal and on the dummy row, or $Y = \text{const}$ line below the body, and using $G_{i,1} = G_{i,3}$ as the end condition or reflecting the variables as is the case for the condition on the correction $\Delta_{i,1}$.

All three cases were run with the same $\alpha$ variation. As shown in Fig. 2, the results are quite sensitive to the boundary condition on the intermediate variable and making the intermediate variable mimic the correction seems to be the best choice. Even with this boundary condition, the YX factorization does not give identical results to the XY factorization and seemed to be somewhat more sensitive to the $\alpha$ variation. Hence, the AF1XY scheme was used for all the computations.

Figure 3 shows a comparison of the convergence rate of the maximum residual for the AF1 and SLOR schemes for a thin subsonic leading-edge elliptic cone ($\theta_c = 20$ deg, $\delta_c = 2$ deg) on a $(48 \times 38)$ cross-flow mesh at $M_\infty = 2$ and angles of attack $\alpha = 0$ and 10 deg. The SLOR scheme found to be optimum for this problem in Ref. 5 is one that sweeps around the body on $Y = \text{const}$ lines. This "column" SLOR scheme was found to be two to five times faster than the alternate SLOR scheme which sweeps toward the body on $Y = \text{const}$ lines. It is also interesting to note that the SLOR scheme for the supersonic freestream problem does not exhibit the typical slowdown in convergence rate that occurs in transonic flow problems after one or two orders of magnitude. A break in the SLOR curve occurs after one order of magnitude but remains linear for further reductions. It is also interesting to note that the SLOR convergence of the $\alpha = 0$ and 10 deg flows are not dramatically different (both taking about 350 to 400 iterations), considering that the 10 deg case is a multishocked flow. At $\alpha = 10$ deg, a strong cross-flow shock develops, but is evidently overshadowed by the convergence of the captured bow shock. The AF1 scheme at $\alpha = 0$ deg converges very quickly. Essentially, these flows are converged when the maximum residual reaches $10^{-2}$. For $\alpha = 0$ deg, this occurs at about 10 iterations or when the log (RESMAX) $= -2$. The AF1 scheme is an order of magnitude faster than the SLOR scheme for $\alpha = 0$ deg. As the angle of attack increases, the AF1 scheme slows down by a factor of 3 while the SLOR remains about the same. Overall, the AF1 scheme is at least three times faster iterationwise than the SLOR scheme. The relaxation factor was 1.5 for these cases in both schemes and three cycles were used in the AF1 scheme. A larger number of cycles did not seem to enhance convergence. Figure 4 shows the surface pressure distributions for the elliptic cone computed in Fig. 3 at $\alpha = 0$, 5, and 10 deg and $M_\infty = 2.0$ on a finer mesh. Both $\alpha = 5$ and 10 deg have cross-flow shocks on the leeward surface.

Before implementing the AF2 scheme, the effect of splitting the transformation derivatives between the two factors was studied. Figure 5 indicates the effect of using different forms for the term $H_m$ in Eq. (16). If the transformation derivatives are neglected in the factorization, the case could only be run when the $\alpha$ variation was increased significantly. Increasing the minimum value of $\alpha$ generally degrades the convergence

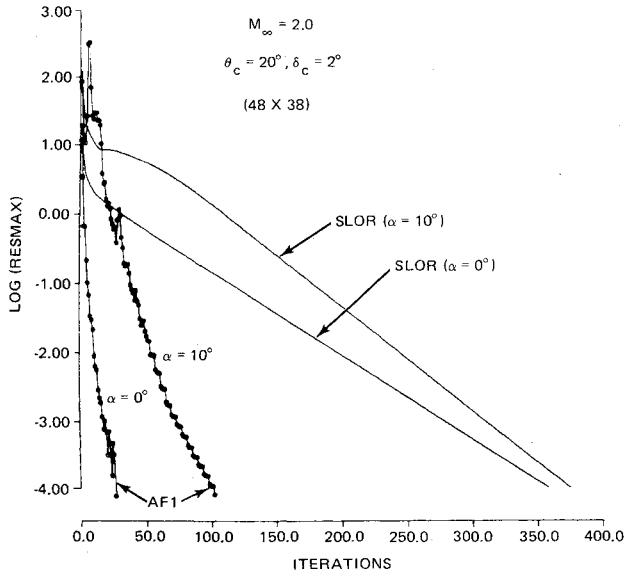


**Fig. 4 Surface pressure distribution for subsonic leading-edge elliptic cone (BSC).**

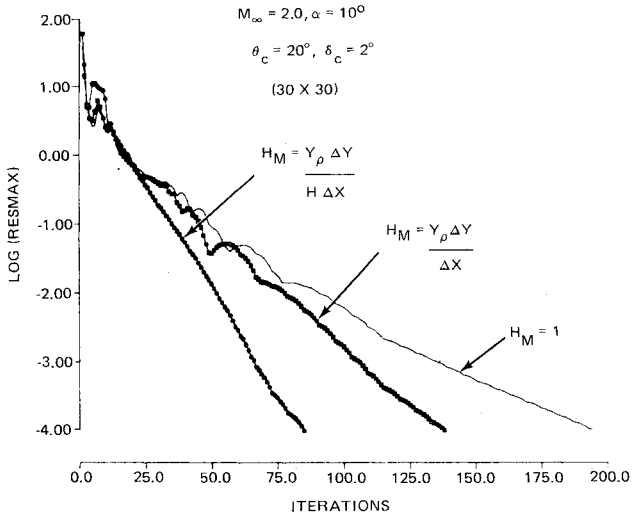


**Fig. 5 The effect of transformation derivatives on the AF2 scheme (BSC).**

rate. The best convergence was achieved when both the metric and shearing transformation derivatives were included in the term $H_m$. The two curves in Fig. 6 with $H_m$ other than unity were obtained with an $\alpha$ variation that diverged when $H_m = 1$. Hence, the AF2 scheme seems to be sensitive to the coordinate transformations and the convergence rate can be affected significantly. The form of $H_m$ is not considered to be optimum and further analytical and numerical studies should be conducted to study its effect on the convergence rate. A nonoptimum $H_m$ may also affect the minimum values of $\alpha$ that can be used.

Figure 6 shows a comparison of the convergence rates of the AF1 and AF2 schemes for the elliptic cone of Fig. 3 at $\alpha = 10$ deg. Comparable convergence rates were achieved for both schemes with the AF2 scheme doing a little better up to $10^{-3}$ and then lagging at the lower tolerances possibly due to a nonoptimum choice of $\alpha$. It was observed that the AF2 scheme convergence rate and stability deteriorated faster than the AF1 scheme for solutions with strong captured bow shocks. This condition generally occurs for elliptic cones that have sonic or supersonic edges. A 30-deg semimajor axis elliptic cone at $M_\infty = 2.0$ and $\alpha = 15$ deg was used to study this effect. For this elliptic cone, a strong multishock flow exists (i.e., embedded cross flow and bow shock).

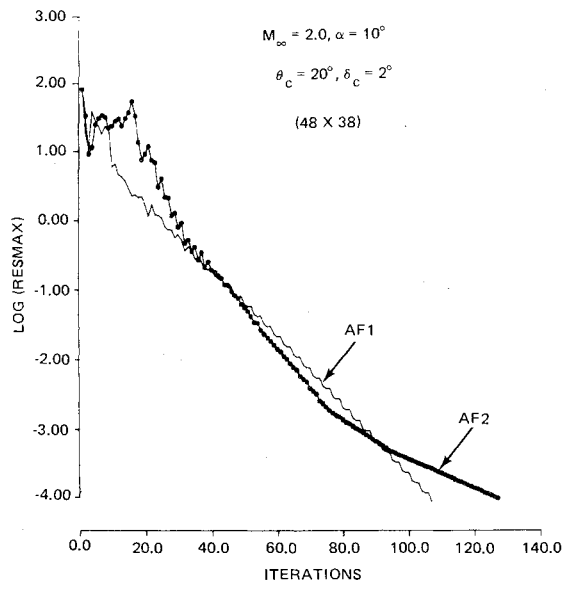


**Fig. 6 Comparison of AF1 and AF2 for a multishock flow (BSC).**

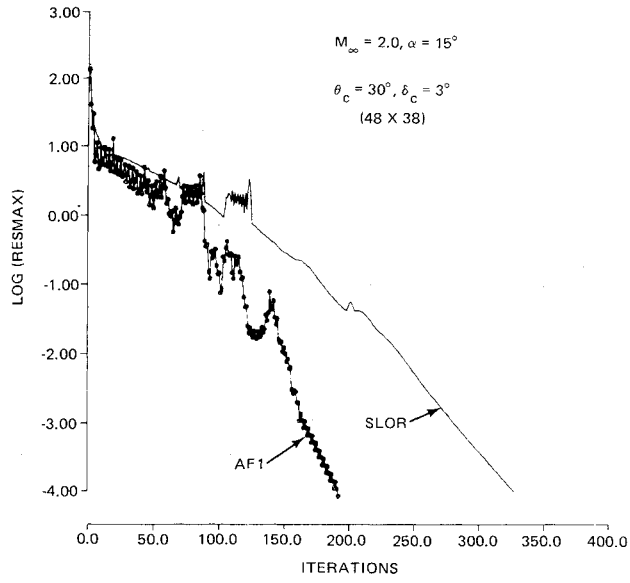


**Fig. 7 Comparison of the AF1 scheme with SLOR for a strong multishock flow (BSC).**

Figure 7 shows a comparison of the AF1 scheme with SLOR. The AF1 scheme barely maintains a factor of two in convergence rate in comparison to SLOR. As indicated in Ref. 4, the SLOR scheme used is optimum for the capture of bow shocks or $Y$ shocks. The only additional gain achieved with the AF1 scheme is a faster propagation in the $X$ direction around the body. Obviously, for this class of flow the bow shock formation dominates the convergence rate. Figure 8 shows the same case for the AF2 scheme in comparison with SLOR. The AF2 scheme does not perform as well as the SLOR scheme. A plot of the average residual shows that the AF2 scheme converges at about the same rate as SLOR. The maximum residual occurs once again at the bow shock. It is suspected that splitting the $Y$ derivative in the AF2 scheme is the major reason for this decline in convergence rate for flows with strong bow shocks. For the case shown in Figs. 7 and 8, the AF2 scheme actually required significantly more temporal damping to maintain stability in comparison with the AF1 scheme. This behavior is different than what has been observed for transonic flows. In transonic flows, typically only one type of shock ($X$ shock) is present in the flow. This is

probably why splitting the $Y$ derivative in transonic flows is not detrimental to the convergence rate.

## Nonconical or Three-Dimensional Flows

The AF1 and AF2 schemes both worked well for quasi-two-dimensional conical flow yielding convergence rates two to ten times faster than SLOR. The AF2 scheme was somewhat more sensitive because of the split $Y$ derivative and the necessity of including the coordinate transformation derivatives in the factorization. Hence, for the present study, the AF1 scheme will be considered for the nonconical or three-dimensional flow problem. Applying the shearing transformation to Eq. (1), the principal terms of the three-dimensional full-potential equation can be rewritten as

$$L(\varphi_{i,j}) = (A_1+B_1)F_{XX} + (A_2+B_2)F_{XY} + (A_3+B_3)F_{YY} + B_8F_{ZZ} + B_9F_{XZ} + B_{10}F_{YZ} + B_{11}F_Z + \ldots \quad (25)$$

where the $B_i$ coefficients represent the additional nonconical $R$ or three-dimensional terms. The $B_i$ coefficients are rather complicated and are defined in Ref. 4.

The geometry is assumed to be conical at the apex or $R=0$ of the configuration. Marching solutions are then obtained on spherical $R$ or $Z=$const surfaces. The terms $F_Z$ and $F_{ZZ}$ always have unwind differences, whereas the $F_{XZ}$ and $F_{YZ}$ terms are smoothly switched when mixed subsonic/supersonic crossflow occurs. A first-order accurate $F_{ZZ}$ difference requires information at two previous planes. Initially, the AF1 scheme was applied to the cross-flow plane $XY$ terms of Eq. (25) with the $Z$ derivatives treated as forcing terms evaluated with old values of the potential. This scheme turned out to be slower and resulted in divergence in many cases when compared to the optimum SLOR which includes all the principal $Z$ terms in the tridiagonal matrix. Hence, a factorization was sought that would maintain the $XY$ cross-flow convergence rate of the AF scheme and still retain the SLOR efficiency for the $Z$ terms. The following AF1Z factorization was proposed for subsonic cross flow, $Q_c^2 < a^2$.

$$\left[\alpha - (A_1+B_1)\frac{\vec{\delta}_X\overleftarrow{\delta}_X}{\Delta X^2} - \frac{B_8}{\Delta Z^2} - \frac{B_9\delta_{Xc}}{2\Delta X\Delta Z} - \frac{B_{11}}{\Delta Z}\right]G^{n+1}_{i,j} = \alpha\omega L(\varphi^n_{i,j})$$

$$\left[\alpha - (A_3+B_3)\frac{\vec{\delta}_Y\overleftarrow{\delta}_Y}{\Delta Y^2} - B_{10}\frac{\delta_{Yc}}{2\Delta Y\Delta Z}\right]\Delta^{n+1}_{i,j} = G^{n+1}_{i,j} \quad (26)$$

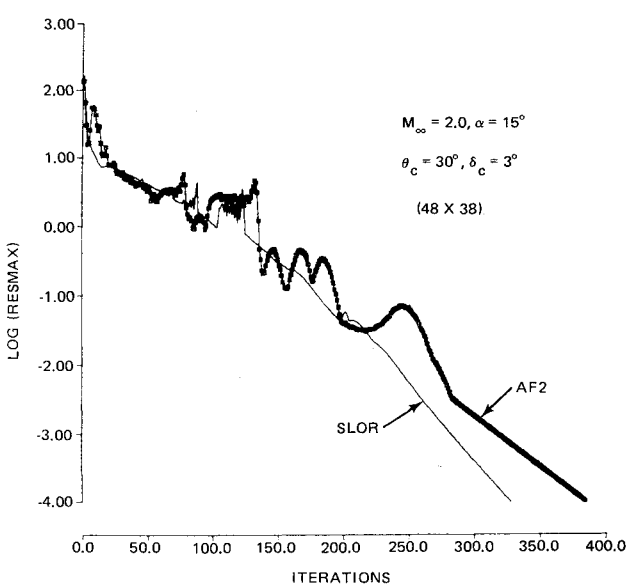


**Fig. 8 Comparison of the AF2 scheme with SLOR for a strong multishock flow (BSC).**

where $\delta_{Xc}$ and $\delta_{Yc}$ represent second-order central first-derivative operators, or

$$\delta_{Xc} = (\ )_{i+1,j} - (\ )_{i-1,j}$$

$$\delta_{Yc} = (\ )_{i,j+1} - (\ )_{i,j-1} \quad (27)$$

The $Z$ terms (e.g., $F_{ZZ}$) do not factor because of the hyperbolic nature of the problem and, hence, are added explicitly to the two factors. The $F_{ZZ}$ difference contains the unknown value of the potential at the current station and the two known values of the potential at the two previous stations. Except for the nonconical coefficients of the $F_{XX}$ and $F_{YY}$ terms, the $Z$ terms are added explicitly to each factor. Including the $Z$ terms in the factorization was also necessary to maintain diagonal dominance and convergence. In many cases, neglecting the $Z$ terms in the AF scheme not only slowed convergence but actually resulted in divergence. For supersonic crossflow, the factorization was modified to include the upwind $Z$ terms or, for $Q_2^2 > a^2$,

$$\left[\alpha - A_{1c}\frac{\vec{\delta}_X\overleftarrow{\delta}_X}{\Delta X^2} - I_s\frac{(A_{1u}+B_1)}{\Delta X^2}(K_1\overleftarrow{\delta}_X - K_2\vec{\delta}_X) - \frac{B_8}{\Delta Z^2} - \frac{B_9}{\Delta X\Delta Z} - \frac{B_{11}}{\Delta Z}\right]G^{n+1}_{i,j} = \alpha\omega L(\varphi^n_{i,j})$$

$$\left[\alpha - A_{3c}\frac{\vec{\delta}_Y\overleftarrow{\delta}_Y}{\Delta Y^2} + (A_{3u}+B_3)\frac{\vec{\delta}_Y}{\Delta Y^2} - B_{10}\frac{\vec{\delta}_Y}{\Delta Y\Delta Z}\right]\Delta^{n+1}_{i,j} = G^{n+1}_{i,j} \quad (28)$$

It was found that the off-diagonal terms of the $F_{XZ}$ derivative could be included in the subsonic cross-flow region but not in the supersonic region leading to the following for the $\delta_{XZ}$ operator for $U>0$, or,

$$\overleftarrow{\delta}_{XZ} = (\ )^{n+1}_{i,j,k} - (\ )^n_{i-1,j,k} - (\ )_{i,j,k-1} + (\ )_{i-1,j,k-1}$$

$$\vec{\delta}_{XZ} = (\ )^n_{i+1,j,k} - (\ )^{n+1}_{i,j,k} - (\ )_{i+1,j,k-1} + (\ )_{i,j,k-1} \quad (29)$$

where the subscript $K$ refers to the present $R$ station and $K-1$ refers to the known values of the potential at the previous station. Hence, care must be taken to preserve the proper balance of new and old values of the potential.

The AF1Z scheme was also found to converge most reliably and optimally if the acceleration parameter $\alpha$ was scaled with $R$, or,

$$\alpha_{\min} = A_{\min}\left(\frac{1}{\Delta X} + \frac{1}{\Delta Y}\right)(1+R)$$

$$\alpha_{\max} = A_{\max}\left(\frac{1}{\Delta X^2} + \frac{1}{\Delta Y^2}\right)(1+R) \quad (30)$$

Hence, the acceleration parameter variation reduces to the conical values at $R=0$ and increases linearly with $R$ as the marching solutions are obtained.

## Three-Dimensional Results

Some preliminary three-dimensional results were obtained using the nonconical AF1Z factorization for three wings of distinctly different geometric character. For these cases, the bow shock fit (BSF) method is used. Typically 20-50 marching steps are used in a computation with no constraints on the size of the marching step except those dictated by accuracy requirements and flowfield details.

Figure 9 illustrates the convergence history of the first case of a highly swept delta wing (Squire wing geometry of Ref. 16) at $M_\infty = 1.80$, $\alpha = 0$ deg. The wing geometry consists of a parabolic centerline thickness distribution with elliptic

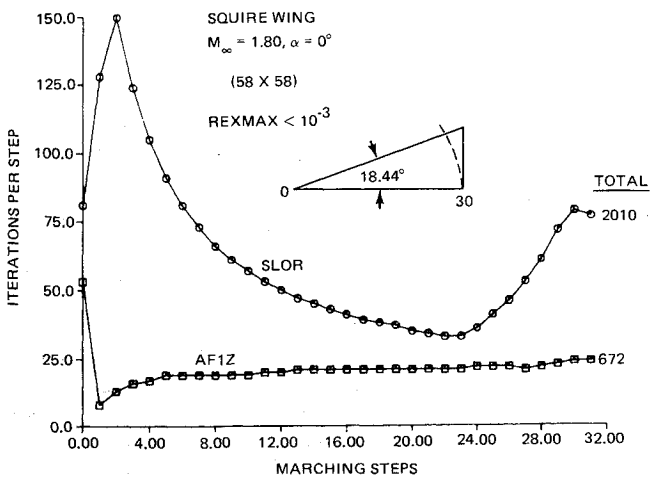


Fig. 9 Squire wing computation, AF1Z vs SLOR (BSF).

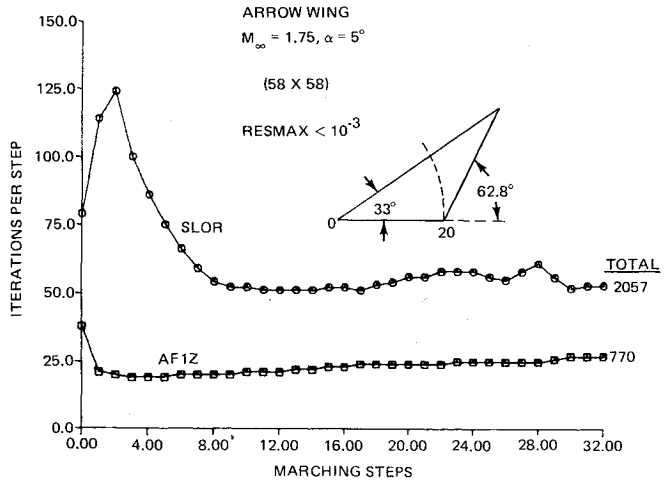


Fig. 10 Arrow wing computation, AF1Z vs SLOR (BSF).

spanwise cross sections. As is the case for most three-dimensional wings, the geometry commences near the apex with a thick (e.g., 3:1 major to minor axis ratio) cross section which becomes thin and eventually approaches a flat-plate cross section at the trailing edge.

Figure 9 shows the number of iterations required per matching step to reduce the maximum residual to $10^{-3}$ (i.e., a minimum of four orders of magnitude) for the SLOR and AF1Z schemes. Step 0 refers to the conical or $R=0$ solution required to start the computation. Fitting the bow shock as the outer boundary reduces the internal flowfield computation to an elliptic problem if an embedded supersonic cross-flow region does not form. For this case, the entire flowfield was elliptic.

Mesh refinement is used only at the conical station and the marching proceeds on the fine mesh. The iterations at step 0 reflect only the fine grid convergence. The AF1Z scheme shows large gains for the initial steps. At the initial steps, the geometry changes most rapidly. The AF1Z gains taper off until the cross section becomes quite thin. The SLOR scheme has some difficulty computing the latter stations in comparison with the AF1Z scheme. Step 30 corresponds to the centerline trailing edge. The calculation is taken beyond the trailing edge in order to compute the entire wing. The wake is assumed to be a flat plate which in this case is an exact assumption. The total iterations for the run are also shown in Fig. 9. The SLOR computation took 2010 fine grid iterations and the AF1Z scheme required only 672 iterations. An overall factor of 3 reduction in iterations was achieved for this case. The actual computation time, which includes geometry and mesh generation, was reduced by a factor of 2.

The next case, shown in Fig. 10, is for a not so highly swept arrow wing at $M_\infty = 1.75$, $\alpha = 5$ deg. The geometry consists of a symmetrical NACA 4% thick four-digit airfoil imposed chordwise on the wing. The wake is approximated as a flat plate. In this calculation, the flowfield becomes supercritical very quickly at $R=3$ or step 4. The same trends apply for this case except that the SLOR scheme does not have any rise in iterations near the trailing edge of the wing. The interesting aspect of the AF1Z scheme is that the nonconical iterations required per step is relatively constant and independent of the geometry variation. Almost a factor of 3 reduction in iterations is again achieved by the AF1Z scheme corresponding to a factor of 2 in running time. Hence, the appearance of supercritical crossflow and a cross-flow shock does not seem to deteriorate the AF1Z scheme significantly. In addition, aft of the trailing edge, the cross-flow shock merges with the trailing-edge shock.

The last case, shown in Fig. 11, is for a realistic supersonic maneuver demonstration wing designed with the aid of NCOREL[17] and built and tested by NASA Langley. Details of

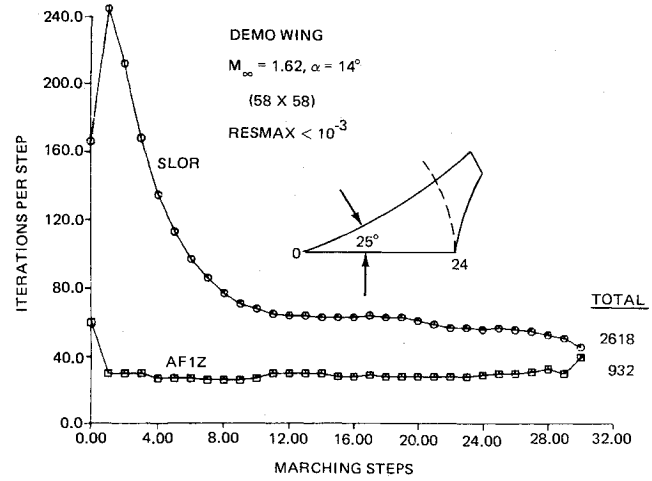


Fig. 11 Demonstration wing computation, AF1Z vs SLOR (BSF).

this wing can be found in Ref. 18. This wing has variable sweep leading and trailing edges. The leading-edge planform angle varies from 25 to 33 deg. The wing also has significant twist and camber. Figure 11 shows the convergence histories for the two schemes at $M_\infty = 1.62$ and $\alpha = 14$ deg. The wake is approximated by a flat-plate extension of the wing spanwise camberline. For this wing, supercritical flow also appears at $R=3$ or step 4. Similar trends apply for this wing except that the AF1Z scheme gains are reduced aft of the trailing edge of the wing. The overall reduction in iterations is similar, being almost a factor of 3 and corresponding to a factor of 2 reduction in running time.

In general, the AF1Z scheme shows great potential in reducing the computational time for three-dimensional computations. Further study of the scaling of the acceleration parameters may result in further gains, since the AF1Z scheme shows a greater reduction at the initial stations and then deteriorates to about a factor of 2. This may be due to improper scaling or choice of acceleration parameters. It should be noted that no temporal damping was used or needed in the AF1Z scheme for the three cases described above.

## Conclusion

Approximate factorization schemes have been applied successfully to the conical supersonic, transonic cross-flow problem and indicate factors of 2-10 reduction in iterations for the bow shock capture method. AF1 and AF2 schemes showed similar convergence rates. The AF2 scheme showed

more sensitivity to the mesh transformations and deteriorated more rapidly with strong captured bow shocks in comparison to the AF1 scheme. Unlike transonic flow, the AF1 scheme proved to be more stable than the AF2 scheme.

The AF1 scheme was then adapted to three-dimensional flow by including the nonconical $Z$ terms explicitly in each factor. Preliminary applications of the AF1Z scheme on a fine grid showed an overall reduction by a factor of 3, iterationwise, and a factor of 2 reduction in running time for wing flowfields.

## References

[1] Siclari, M. J., "Investigation of Crossflow Shocks on Delta Wings in Supersonic Flow," *AIAA Journal*, Vol. 18, Jan. 1980, p. 85.

[2] Grossman, B., "Numerical Procedure for the Computation of Irrotational Conical Flows," *AIAA Journal*, Vol. 17, Aug. 1979, p. 828.

[3] Jameson, A., "Iterative Solution of Transonic Flow over Airfoils and Wings, Including Flows at Mach 1," *Communications on Pure and Applied Mathematics*, Vol. 27, May 1974, pp. 283-309.

[4] Grossman, B. and Siclari, M. J., "Nonlinear Supersonic Potential Flow Over Delta Wings," *AIAA Journal*, Vol. 19, May 1981, p. 573.

[5] Siclari, M. J., "Supersonic Nonlinear Potential Flow with Implicit Isentropic Shock Fitting," *AIAA Journal*, Vol. 20, July 1982, p. 924.

[6] Shankar, V., "An Implicit Marching Procedure for the Treatment of Supersonic Flow Fields using the Conservative Full Potential Equation," AIAA Paper 81-1004, June 1981.

[7] Shankar, V., Osher, S., and Jones, K., "An Efficient Full Potential Implicit Method Based on Characteristics for Analysis of Supersonic Flows," AIAA Paper 82-0974, 1982.

[8] Sritharan, S. S. and Seebass, A. R., "A Finite Area Method for Nonlinear Conical Flows," AIAA Paper 82-0995, 1982.

[9] Peaceman, D. W. and Rachford, H. H., "The Numerical Solution of Parabolic and Elliptic Differential Equations," *Journal of the Society of Industrial and Applied Mechanics*, Vol. 3, 1955, pp. 28-41.

[10] Ballhaus, W. F., Jameson, A., and Albert, J., "Implicit Approximate Factorization Schemes for the Efficient Solution of Steady Transonic Flow Problems," *AIAA Journal*, Vol. 16, June 1978, pp. 573-579.

[11] Holst, T. L., "Fast Conservative Algorithm for Solving the Transonic Full-Potential Equation," *AIAA Journal*, Vol. 18, Dec. 1980, pp. 1431-1439.

[12] Baker, T. J., "A Fast Implicit Algorithm for the Nonconservative Potential Equation," Open Forum Presentation at the AIAA 4th Computational Fluid Dynamics Conference, July 1979.

[13] Baker, T. J., "Potential Flow Calculation by the Approximate Factorization Method," *Journal of Computational Physics*, Vol. 42, 1981, pp. 1-19.

[14] Catherall, D., "Optimum Approximate-Factorization Schemes for 2D Steady Potential Flows," AIAA Paper 81-1018, June 1981.

[15] Jameson, A., "Acceleration of Transonic Potential Flow Calculations on Arbitrary Meshes by the Multiple Grid Methods," AIAA Paper 79-1458, July 1979.

[16] Weber, J. and King, C., "Analysis of the Zero-Lift Drag Measured in Delta Wings," ARC R&M 3818, June 1976.

[17] Siclari, M. J., "The NCOREL Computer Program for 3D Nonlinear Supersonic Potential Flow Computations," NASA CR-3694, Aug. 1983.

[18] Mason, W. H., Miller, D. S., Pittman, J. L., and Siclari, M. J., "A Supersonic Maneuver Wing Designed for Nonlinear Attached Flow," AIAA Paper 83-0425, Jan. 1983.